Influence of Doubled CO_2 on Ozone via Changes in the Brewer–Dobson Circulation

XUN JIANG

Division of Geological and Planetary Sciences, and Department of Environmental Science and Engineering, California Institute of Technology, Pasadena, California

SCOTT J. EICHELBERGER AND DENNIS L. HARTMANN

Department of Atmospheric Sciences, University of Washington, Seattle, Washington

RUNLIE SHIA AND YUK L. YUNG

Division of Geological and Planetary Sciences, California Institute of Technology, Pasadena, California

(Manuscript received 8 February 2006, in final form 7 November 2006)

ABSTRACT

In this short note, the effect of enhanced circulation due to doubling CO_2 on ozone is investigated. The difference of Brewer–Dobson circulation (BDC) between the doubled CO_2 and control run from an idealized atmospheric general circulation model is added to the BDC climatology derived from National Centers for Environmental Prediction—Department of Energy Reanalysis 2 (NCEP2) from 1979 to 2002. Then it is used to drive the California Institute of Technology/Jet Propulsion Laboratory (Caltech/JPL) two-dimensional chemistry and transport model. The results reveal that the total ozone increases by 7 and 3.5 Dobson units (DU) in the high latitudes of the Northern and Southern Hemispheres, respectively, and decreases by 4 DU in the Tropics as a result of the increase in BDC associated with doubled CO_2. If the change of eddy mixing coefficients after doubling CO_2 is also considered, the total ozone will increase by 6.5 and 3 DU in the high latitudes of the Northern and Southern Hemispheres after combining both effects from the change in BDC and eddy mixing coefficients.

Recent general circulation model (GCM) studies (Rind et al. 1998, 2002; Butchart and Scaife 2001; Sigmond et al. 2004; Butchart et al. 2006) suggest that the strength of the Brewer–Dobson circulation (BDC) increases due to CO_2-induced global warming. Using an atmospheric GCM (AGCM), Eichelberger and Hartmann (2005) have demonstrated that an increase in the BDC can be produced by the increased temperature gradient between Tropics and extratropics associated with global warming in GCMs. In this note, we will investigate the influence of enhanced BDC and eddy mixing coefficients because of doubled CO_2 on the column ozone. First, we will calculate the difference of BDC and eddy mixing coefficients from the double CO_2 and control runs from Eichelberger and Hartmann (2005). Then the difference of BDC and eddy mixing coefficients will be used to drive Caltech/JPL two-dimension (2D) chemistry and transport model (CTM).

The AGCM from Eichelberger and Hartmann (2005) solves the dry hydrostatic primitive equations. It is T21 (triangular wavenumber truncation at 21) resolution in the horizontal and 50 levels evenly spaced in log pressure from the surface to approximately 10^{-3} hPa. The bottom boundary of the model is flat. Forcing in the model is applied via Newtonian relaxation of temperature to a prescribed zonally symmetric radiative equilibrium temperature field. To qualitatively simulate a doubled CO_2 climate, a zonally symmetric tropical heat source is introduced into the model. The tropical warming causes the midlatitude baroclinicity to increase, which leads to an increase in the wave activity at synoptic and planetary scales (Eichelberger and Hartmann 2005). The model is run under perpetual January conditions with no stationary wave forcing. Preliminary results indicate that the change caused by tropical warming is similar for the case with and without stationary

Corresponding author address: Xun Jiang, California Institute of Technology, 150-21, Pasadena, CA 91106.
E-mail: xun@gps.caltech.edu

DOI: 10.1175/JAS3969.1

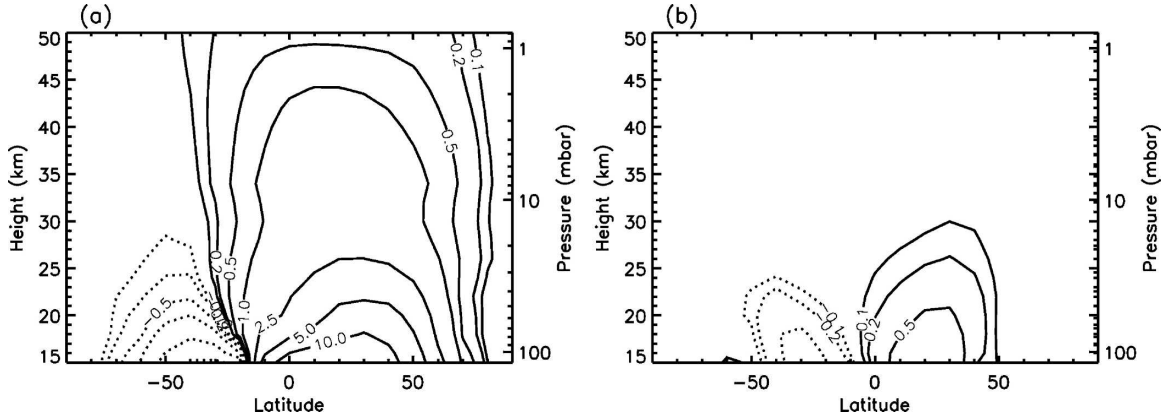

FIG. 1. (a) Standard NCEP2 streamfunction for January in the stratosphere (Jiang et al. 2004). (b) Streamfunction difference between the double CO_2 and control runs (Eichelberger and Hartmann 2005). Units are 10^9 kg s^{-1}.

waves. This verifies that the BDC in the stratosphere increases in response to baroclinically forced planetary waves.

Using the meridional wind, temperature, and surface pressure data from the double CO_2 and control runs from Eichelberger and Hartmann (2005), we calculate the difference of the BDC through the new method described in Jiang et al. (2004). This method has been successfully used to simulate the interannual variability of column ozone in the Tropics from 1979 to 2002. First, we calculate the 3D meridional mass flux by the vertical integral of meridional wind on the pressure surfaces. Then we interpolate the 3D meridional mass flux to isentropic surfaces, using a mass-conserving linear interpolation scheme (Juckes et al. 1994). The 2D isentropic mass streamfunction $\psi_\theta(\varphi, \theta)$ is derived by zonal averaging of the 3D isentropic meridional mass flux, $\psi_\theta(\lambda, \varphi, \theta)$, along isentropes. Finally, we interpolate the 2D isentropic mass streamfunction $\psi_\theta(\varphi, \theta)$ to the pressure coordinates to produce the pressure surface streamfunction, $\psi_P(\varphi, p)$ so that it can be used to drive the Caltech/JPL 2D CTM.

The mean pressure surface streamfunction in January derived from National Centers for Environmental Prediction—Department of Energy Reanalysis 2 (NCEP2) (Kanamitsu et al. 2002) from 1979 to 2002 is shown in Fig. 1a. The NCEP does not have data above 40 km, where we adopt the climatologically averaged circulation derived by Fleming et al. (2002) for the Goddard Space Flight Center (GSFC) 2D model. There is a gradual merging of the two between 30 and 40 km. The total upwelling mass flux is about 17.8×10^9 kg s^{-1} at 100 hPa for the mean pressure surface streamfunction. The total upwelling mass flux is defined as the sum of all upwelling flux at 100 hPa. The difference of the stream functions between the double CO_2 and control runs from Eichelberger and Hartmann (2005) in January is shown in Fig. 1b. Upwelling (downwelling) increases in the Tropics (high latitude) region for the doubled CO_2 temperature change. The increase in downwelling extends outside the polar region into midlatitudes. The total upwelling mass flux anomaly at 100 hPa is about 1.72×10^9 kg s^{-1}, which is about 9.7% of that in the climatology.

In addition to changing the strength of the BDC, the doubled CO_2 will also influence the eddy mixing coefficients. The isentropic mixing coefficient, K_{yy}, can be related to the Eliassen–Palm flux divergence (Tung 1986; Yang et al. 1990). Figure 2a shows the K_{yy} field on the pressure surfaces in January from Fleming et al. (2002); K_{yy} is larger in the NH than in the SH, as a result of more wave activity in the NH. The difference of K_{yy} derived between the double CO_2 and control runs from Eichelberger and Hartmann (2005) is shown in Fig. 2b. There is enhanced eddy mixing coefficients in the midlatitudes after doubling CO_2.

The differences of the stream functions and the eddy mixing coefficients are added to the climatology streamfunction and K_{yy} in January. The enhanced circulation and eddy mixing coefficients will be used to drive the 2D Caltech/JPL CTM. The 2D CTM is a zonally averaged model for trace species in the terrestrial troposphere and middle atmosphere (Shia et al. 1989; Morgan et al. 2004; Jiang et al. 2004). The model has 18 latitude boxes, equally spaced from pole to pole, and 40 layers, equally spaced in $\log(p)$ from the surface to the upper boundary at 0.01 mbar. The model includes all the gas phase chemistry in the National Aeronautics and Space Administration (NASA) recommendations for stratospheric modeling (DeMore et al. 1997). Heterogeneous chemistry is not included. The numerical method used for solving the continuity equation in the

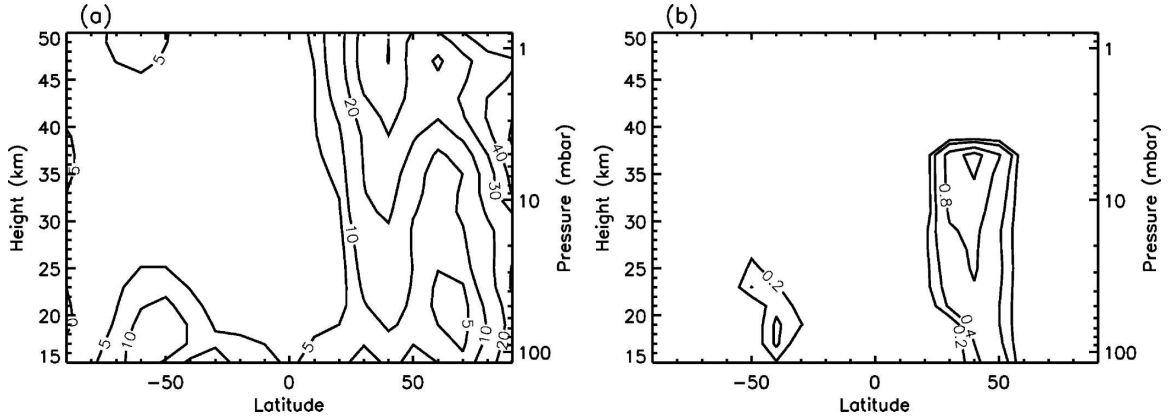

FIG. 2. (a) Isentropic mixing coefficient K_{yy} for January from Fleming et al. (2002). (b) Isentropic mixing coefficient K_{yy} difference between the double CO_2 and control runs from Eichelberger and Hartmann (2005). Units are 10^9 cm^2 s^{-1}.

model is the Prather scheme (Prather 1986; Shia et al. 1990). Important features of the Caltech/JPL 2D CTM include its ability to reproduce the age of air based on CO_2 and SF_6 measurements in the stratosphere and the observed climatology of O_3 (see appendix A of Morgan et al. 2004). Transport in the model is by the streamfunction, horizontal eddy diffusivity K_{yy}, and vertical diffusivity K_{zz}. The values for K_{zz} are taken from Summers et al. (1997); they are not important except in the mesosphere.

To understand the influence of doubled CO_2 on ozone, four experiments are carried out. Details for these experiments are listed in Table 1. In experiment A, we use the streamfunction from NCEP2 and K_{yy} from Fleming et al. (2002) to drive the 2D CTM. In experiment B, we use the enhanced streamfunction and the same K_{yy} as in experiment A. In experiment C, we use the enhanced eddy mixing coefficient K_{yy} and NCEP2 streamfunction. In experiment D, we use both enhanced streamfunction and enhanced eddy mixing coefficients. The ozone difference between experiment B and A is purely due to the strengthening of the BDC.

TABLE 1. Description of model runs.

Model run	Description
Experiment A	Streamfunction from NCEP2 and K_{yy} from Fleming et al. (2002)
Experiment B	Enhanced streamfunction and same K_{yy} as experiment A
Experiment C	Streamfunction from NCEP2 and enhanced K_{yy}
Experiment D	Enhanced streamfunction and enhanced K_{yy}
Experiment E	Same streamfunction and K_{yy} as experiment A, O_3 is not transported.
Experiment F	Enhanced streamfunction and enhanced K_{yy}, O_3 is not transported.

The result for column ozone is shown as the solid line in Fig. 3. Negative ozone anomalies occur throughout the Tropics, and positive anomalies occur in the middle and high latitudes. The maximum value is about 7 and 3.5 Dobson units (DU, where 1 DU is the equivalent of 2.69×10^{16} molecules of ozone per square centimeter) in the high latitudes of the Northern and Southern Hemispheres, respectively. The difference between experiment C and A is shown as the dashed line in Fig. 3. The enhanced eddy mixing coefficients reduces the gradient between the pole and the equator. It creates a positive anomaly in the Tropics and negative anomalies in the high latitudes. The eddy mixing coefficient effect is smaller than the streamfunction effect. The difference between experiments D and A reveals that the net effect from streamfunction and eddy mixing coefficients is about 6.5 and 3 DU increase in the column ozone in the high latitudes for the Northern and Southern Hemispheres, respectively. The tropical ozone decreases ~4 DU as response to the doubling CO_2. This

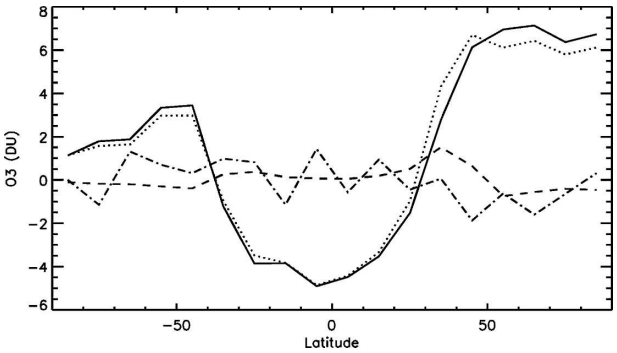

FIG. 3. Column ozone difference between experiments B and A (solid line), experiments C and A (dashed line), experiments D and A (dotted line), and experiments F and E (dash–dot line).

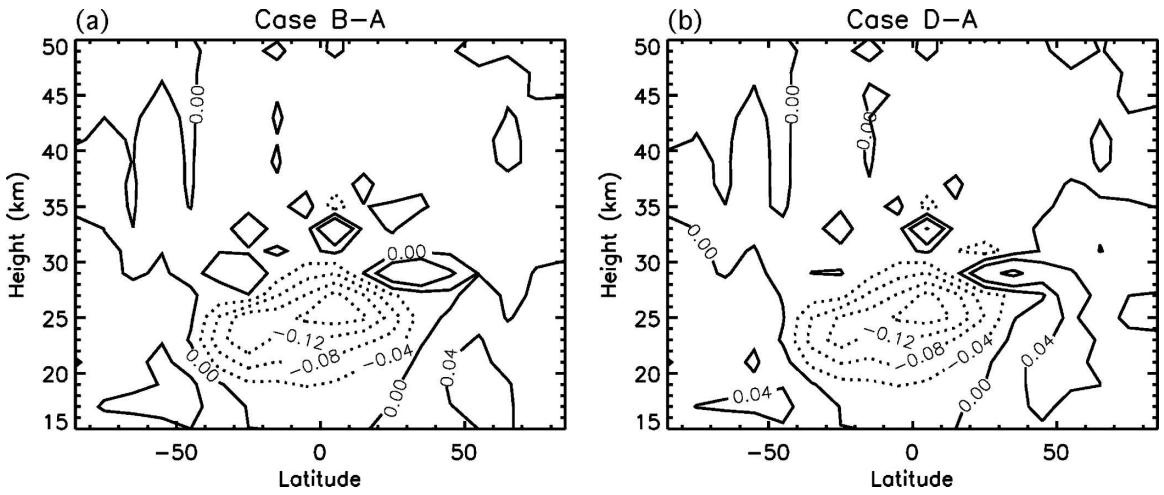

FIG. 4. Ozone mixing ratio difference between (a) experiments B and A, and (b) experiments D and A.

result is mostly due to the direct transport of ozone, as the column ozone is dominated by the ozone below 35 km, where ozone is mainly dynamically controlled (Ko et al. 1989).

The effect of the transport of long-lived gases that are sources for the ozone photochemical loss is smaller compared with the dynamical effect. To reveal that, we carried out two more experiments. In experiments E, we use the same streamfunction and K_{yy} as experiment A. However, ozone is not transported in experiment E. In experiment F, we use the enhanced streamfunction and enhanced K_{yy}. Ozone is still not transported. The difference of experiments F and E, shown as the dash–dot line in Fig. 3, represents the effect of the transport of long-lived gases. This effect is smaller compared with that from direct transport of ozone.

Ozone mixing ratio difference between experiments B and A are shown in Fig. 4a. The ozone depletion is mainly in 18–30 km in the Tropics and midlatitudes. More ozone is transported to the high latitudes. As a result, the total ozone as a minimum in the Tropics and maximum in the high latitudes. Ozone mixing ratio difference between experiments D and A (Fig. 4b) combine both effect from streamfunction and eddy mixing coefficients. The result in Fig. 4b is very similar to that in Fig. 4a, which suggests that most effect is from direct transport of ozone.

In this work, we have restricted our interest to the influence of doubled CO_2 on the BDC and eddy mixing coefficients, and their consequences on the ozone distribution. Additional changes as a result of the change of the chemical reaction rates due to stratospheric cooling and the presence of polar stratospheric clouds (PSCs) have been investigated by Shindell et al. (1998a,b). However, the effects of the changes of BDC and ozone have not been isolated, and would have been difficult given the large variability of the seasonal cycle in a GCM.

In summary, the strengthening of the BDC due to the doubling of CO_2 appears to be a robust result (Rind et al. 1998, 2002; Butchart and Scaife 2001; Sigmond et al. 2004; Eichelberger and Hartmann 2005; Butchart et al. 2006). According to Eichelberger and Hartmann (2005), the BDC increases by ~10% in the winter, causing as much as 7 and 3.5 DU of increase in ozone column at high latitudes for the Northern and Southern Hemispheres, respectively. It is an important result to be considered in the modeling of ozone recovery. If we also include the strengthening of the eddy mixing coefficients, it will lead to the 6.5- and 3-DU increase in high-latitude column ozone for the Northern and Southern Hemispheres, respectively. The effect of the transport of long-lived gases that are sources for the ozone photochemical loss is smaller compared with the dynamical effect. Further study is needed to help us understand the synergistic interaction between ozone change and climate variability, and its influence on the ozone recovery.

Acknowledgments. This work was supported by NASA Grant NNG04GD76G to the California Institute of Technology, and by the Climate Dynamics Program of the National Science Foundation under Grant ATM-0409075 to the University of Washington.

REFERENCES

Butchart, N., and A. A. Scaife, 2001: Removal of chlorofluorocarbons by increased mass exchange between the stratosphere and troposphere in a changing climate. *Nature,* **410,** 799–802.

——, and Coauthors, 2006: Simulations of anthropogenic change

in the strength of the Brewer–Dobson circulation. *Climate Dyn.,* **27,** 727–741.

DeMore, W. B., and Coauthors, 1997: Chemical kinetics and photochemical data for use in stratospheric modeling. JPL Publication 97-4, Jet Propulsion Laboratory, Pasadena, CA, 269 pp.

Eichelberger, S. J., and D. L. Hartmann, 2005: Changes in the strength of the Brewer-Dobson circulation in a simple AGCM. *Geophys. Res. Lett.,* **32,** L15807, doi:10.1029/2005GL022924.

Fleming, E. L., C. H. Jackman, J. E. Rosenfield, and D. B. Considine, 2002: Two-dimensional model simulations of the QBO in ozone and tracers in the tropical stratosphere. *J. Geophys. Res.,* **107,** 4665, doi:10.1029/2001JD001146.

Jiang, X., C. D. Camp, R. Shia, D. Noone, C. Walker, and Y. L. Yung, 2004: Quasi-biennial oscillation and quasi-biennial oscillation–annual beat in the tropical total column ozone: A two-dimensional model simulation. *J. Geophys. Res.,* **109,** D16305, doi:10.1029/2003JD004377.

Juckes, M. N., I. N. James, and M. Blackburn, 1994: The influence of Antarctica on the momentum budget of the southern extratropics. *Quart. J. Roy. Meteor. Soc.,* **120,** 1017–1044.

Kanamitsu, M., W. Ebisuzaki, J. Woollen, S.-K. Yang, J. J. Hnilo, M. Fiorino, and G. L. Potter, 2002: NCEP–DOE AMIP-II Reanalysis (R-2). *Bull. Amer. Meteor. Soc.,* **83,** 1631–1643.

Ko, M. K. W., N. Sze, and D. K. Weisenstein, 1989: The roles of dynamical and chemical processes in determining the stratospheric concentration of ozone in one-dimensional and two-dimensional models. *J. Geophys. Res.,* **94,** 9889–9896.

Morgan, C. G., M. Allen, M. C. Liang, R. L. Shia, G. A. Blake, and Y. L. Yung, 2004: Isotopic fractionation of nitrous oxide in the stratosphere: Comparison between model and observations. *J. Geophys. Res.,* **109,** D04305, doi:10.1029/2003JD003402.

Prather, M. J., 1986: Numerical advection by conservation of second-order moments. *J. Geophys. Res.,* **91,** 6671–6681.

Rind, D., D. Shindell, P. Lonergan, and N. K. Balachandran, 1998: Climate change and the middle atmosphere. Part III: The doubled CO_2 climate revisited. *J. Climate,* **11,** 876–894.

——, P. Lonergan, N. K. Balachandran, and D. Shindell, 2002: $2 \times CO_2$ and solar variability influences on the troposphere through wave-mean flow interactions. *J. Meteor. Soc. Japan,* **80,** 863–876.

Shia, R.-L., Y. L. Yung, M. Allen, R. W. Zurek, and D. Crisp, 1989: Sensitivity study of advection and diffusion coefficients in a two-dimensional stratospheric model using excess carbon 14 data. *J. Geophys. Res.,* **94,** 18 467–18 484.

——, Y. L. Ha, J.-S. Wen, and Y. L. Yung, 1990: Two-dimensional atmospheric transport and chemistry model: Numerical experiments with a new advection algorithm. *J. Geophys. Res.,* **95,** 7467–7483.

Shindell, D. T., D. Rind, and P. Lonergan, 1998a: Climate change and the middle atmosphere. Part IV: Ozone response to doubled CO_2. *J. Climate,* **11,** 895–918.

——, ——, and ——, 1998b: Increased polar stratospheric ozone losses and delayed eventual recovery owing to increasing greenhouse-gas concentrations. *Nature,* **392,** 589–592.

Sigmond, M., P. C. Siegmund, E. Manzini, and H. Kelder, 2004: A simulation of the separate climate effects of middle-atmospheric and tropospheric CO_2 doubling. *J. Climate,* **17,** 2352–2367.

Summers, M. E., D. E. Siskind, J. T. Bacmeister, R. R. Conway, S. E. Zasadil, and D. F. Strobel, 1997: Seasonal variation of middle atmospheric CH_4 and H_2O with a new chemical-dynamical model. *J. Geophys. Res.,* **102,** 3503–3526.

Tung, K. K., 1986: Nongeostrophic theory of zonally averaged circulation. Part I: Formulation. *J. Atmos. Sci.,* **43,** 2600–2618.

Yang, H., K. K. Tung, and E. Olaguer, 1990: Nongeostrophic theory of zonally averaged circulation. Part II: Eliassen–Palm flux divergence and isentropic mixing coefficient. *J. Atmos. Sci.,* **47,** 215–241.